

Transferrin receptor modulated by microRNA-497-5p suppresses cervical cancer cell malignant phenotypes

Xiangming Fang^{A,E}, Pei Hu^B, Ying Gao^C, Chuqiao Chen^C, Jianqing Xu^D

Department of Gynecology, Shulan (Hangzhou) Hospital, Shulan International Medical College, Zhejiang Shuren University, Hangzhou, China

A – research concept and design; B – collection and/or assembly of data; C – data analysis and interpretation;

D – writing the article; E – critical revision of the article; F – final approval of the article

Advances in Clinical and Experimental Medicine, ISSN 1899–5276 (print), ISSN 2451–2680 (online)

Adv Clin Exp Med. 2024;33(3):273–282

Address for correspondence

Xiangming Fang

E-mail: fang08_12xm@163.com

Funding sources

None declared

Conflict of interest

None declared

Received on October 21, 2022

Reviewed on January 29, 2023

Accepted on June 14, 2023

Published online on July 24, 2023

Abstract

Background. Cervical cancer is prevalent throughout the world, and microRNA-497-5p (miR-497-5p) plays an important role in its development. However, the specific mechanism by which miR-497-5p targets the transferrin receptor (TFRC) during cervical cancer development has not been clarified.

Objectives. The aim of the study was to unravel TFRC expression and its role in cervical cancer cells, as well as the impact of the miR-497-5p/TFRC axis on cervical cancer cells.

Materials and methods. The target mRNA was determined through differential analysis, followed by the evaluation of its impact on survival and clinical staging. Then, quantitative real-time polymerase chain reaction (qPCR) was conducted to analyze the TFRC mRNA level in cervical cancer cells and normal cervical epithelial cells. Western blot (WB) was utilized to examine the expression levels of TFRC, cleaved caspase-3, cleaved caspase-9, and epithelial–mesenchymal transition (EMT)-related proteins. The miRNAs upstream of the target mRNA were predicted, and Pearson correlation analysis was performed, followed by the validation through the dual-luciferase reporter assay. The 3-(4,5-dimethylthiazol-2-yl)-2,5-diphenyltetrazolium bromide (MTT) and colony formation assays were performed to analyze cancer cell viability, followed by a transwell assay aimed at measuring cell migratory and invasive abilities. Finally, flow cytometry was conducted to examine cell apoptosis and cell cycle.

Results. The transferrin receptor was significantly increased in cervical cancer cells and positively associated with clinical T and N stages. Silencing TFRC could constrain cell proliferative, migratory and invasive abilities, arrest the cell cycle and facilitate cell apoptosis in cervical cancer cells. The bioinformatics analysis showed a significantly negative correlation between miR-497-5p and TFRC in cervical cancer. Moreover, upregulated miR-497-5p hampered cervical cancer progression and decreased TFRC expression. The overexpression of TFRC reversed the suppressive impact of miR-497-5p overexpression on cervical cancer progression.

Conclusions. The modulatory role of the miR-497-5p/TFRC axis was confirmed in cervical cancer cells. This axis may present a new avenue for the diagnosis of cervical cancer and provide a novel target for cervical cancer treatment.

Key words: miR-497-5p, TFRC, biological function, cervical cancer

Cite as

Fang X, Hu P, Gao Y, Chen C, Xu J. Transferrin receptor modulated by microRNA-497-5p suppresses cervical cancer cell malignant phenotypes. *Adv Clin Exp Med.* 2024;33(3):273–282. doi:10.17219/acem/168342

DOI

10.17219/acem/168342

Copyright

Copyright by Author(s)

This is an article distributed under the terms of the Creative Commons Attribution 3.0 Unported (CC BY 3.0) (<https://creativecommons.org/licenses/by/3.0/>)

Background

Cervical cancer is a gynecological malignancy with increasing morbidity and mortality worldwide, especially in developing countries.¹ In China, cervical cancer mortality ranks 4th among all cancers, and 2nd among cancers in women. Furthermore, it is commonly reported in patients aged 40–50 years old in China,² and there are approx. 500,000 newly diagnosed cervical cancer cases each year.³ Cervical cancer may be induced by a variety of modalities⁴ and may develop complications during its progression,⁵ making its treatment complex and difficult. Although novel diagnostic and therapeutic technologies for cervical cancer are underpinned by extensive clinical research,⁶ leading to a 30–50% 5-year survival rate in patients at advanced stages,⁷ the therapeutic efficacy is still poor due to tumor recurrence and metastasis.⁸ Therefore, further investigation of effective targets for cervical cancer treatment is warranted.

The transferrin receptor (*TFRC*), namely CD71, participates in iron homeostasis and cell growth,^{9,10} and TfR1 is often upregulated in tissue with a high proliferation index.¹¹ The TfR1/CD71 is overexpressed in several human malignancies, such as lymphoma, liver cancer,¹² colon cancer,¹³ and endometrial cancer,¹⁴ and may be associated with tumor stage and progression.¹¹ The iron uptake by *TFRC* is an essential approach for cellular iron absorption, and *TFRC* is significantly dysregulated in many malignant cell types.¹⁵ However, the expression of *TFRC* in cervical cancer as well as its molecular mechanism are still not fully understood.

Aberrantly expressed microRNAs (miRNAs) are associated with tumorigenesis.¹⁶ Some miRNAs can act as oncogenes to promote tumorigenesis, while others serve as tumor suppressor genes.^{17,18} Numerous studies have demonstrated that miRNAs are a new class of tumor markers for cancer diagnosis, therapy and prognosis.¹⁹ A previous study²⁰ unveiled that miRNAs repressed target gene expression by interfering with the genes or inhibiting mRNA translation. Accordingly, understanding the targets and regulatory mechanisms of miRNAs contributes to easier application of miRNAs in the cancer field. Recently, microRNA-497-5p (miR-497-5p) has been shown to be aberrantly expressed in several different cancers.^{21–23} For example, miR-497-5p modulates FGF2 to hamper proliferative and invasive properties of non-small cell lung cancer (NSCLC).²⁴ Moreover, Zheng et al. proposed that miR-497-5p targeted HMGA2 to hinder hepatocellular carcinoma cell proliferation and metastasis.²⁵ Furthermore, miR-497-5p/PDK3 restrains gastric cancer cell proliferation and cell cycle.²⁶ However, the molecular mechanism of miR-497-5p in cervical cancer is lacking, and together with the lack of a targeted treatment represents an urgent research need.

Objectives

The aim of this study was to explore the mechanism of miR-497-5p and its ability to modulate *TFRC* in cervical cancer. The findings will contribute to the application of miR-497-5p/*TFRC* in cervical cancer diagnosis and prognosis.

Materials and methods

Bioinformatics methods

Expression profiles of mature miRNAs (normal: 3, tumor: 309) and mRNAs (normal: 3, tumor: 306) as well as clinical data from cervical cancer patients were obtained from The Cancer Genome Atlas (TCGA) database. The “edgeR” package was employed for a differential analysis of miRNAs and mRNAs between normal and tumor groups ($|\log FC| > 1.5$, $p_{adj} < 0.05$), allowing for the determination of differentially expressed miRNAs (DEmiRNAs) and mRNAs (DEmRNAs). The target mRNA was selected according to previous literature.^{27,28} Pearson correlation analysis was conducted to determine upstream miRNA, and upstream regulatory miRNAs of the target mRNA were identified using starBase, TargetScan and mirDIP databases. Finally, the survival analysis was carried out on the target mRNA by using the “survival” package in R. The relationship between the clinical stage and differential gene expression of miRNA was also analyzed.

Cell culture

Human normal cervical epithelial cell line HcerEpic (BNCC340374), and 4 human cervical cancer cell lines, namely Hela (BNCC337633), SiHa (BNCC102118), Caski (BNCC338223), and C33A (BNCC341097) were accessed from BeNa Culture Collection (Beijing, China). The HcerEpic, SiHa and C33A cells were cultured in Dulbecco's modified Eagle medium (DMEM) (Gibco, Grand Island, USA) with 10% fetal bovine serum (FBS) (Gibco), while the other cervical cells were kept in RPMI-1640 medium with 10% FBS. Penicillin and streptomycin were added to all the media, and all cultures were maintained with 5% CO₂ at 37°C.

Cell transfection

The sh-*TFRC* (*TFRC* knockdown treatment) and sh-NC (control of *TFRC* knockdown), as well as pcDNA3.1-constructed oe-*TFRC* (*TFRC* overexpression treatment) and oe-NC (control of *TFRC* overexpression) plasmids were procured from GeneChem (Shanghai, China). Lipofectamine™ RNAiMAX (cat. No. 13778150; Invitrogen, Waltham, USA) was applied to perform the cell transfection. A miR-497-5p mimic (miR-497-5p overexpression

treatment) and NC-mimic (control of miR-497-5p overexpression) (GenePharma, Suzhou, China) were transfected into cervical cancer cells with Lipofectamine™ 2000 (cat. No. 11668019; Invitrogen). Samples were cultured for 2 days in the corresponding medium at 37°C with 5% CO₂. After culture, transfection efficiency was detected using quantitative real-time polymerase chain reaction (qPCR).

qPCR

The *miR-497-5p* and *TFRC* mRNA expression levels in cervical cancer cells were assayed using qPCR. The TRIzol reagent (Thermo Fisher Scientific, Waltham, USA) was utilized for total RNA extraction, and the total RNA concentration was assessed with a NanoDrop ND-1000 instrument (NanoDrop Technologies, Wilmington, USA). Specific primers (RiboBio, Guangzhou, China) and prime script RT reagent kit (Takara, Kusatsu, Japan) were employed to reverse transcribe miRNA and mRNA into cDNA. Next, SYBR-Green PCR kit (Applied Biosystems, Waltham, USA) and SYBR® Premix Ex Taq™ II kit (Takara) were employed to quantify miRNA and mRNA expression, respectively. Finally, qRT-PCR was conducted on an ABI Prism 7500 fast real-time PCR system (Applied Biosystems). Endogenous references for *miR-497-5p* and *TFRC* were *U6* and *GAPDH*, respectively. The 2^{-ΔΔC_t} method was utilized to quantify and compare relative expression levels of miR-497-5p or TFRC mRNA in control and experiment groups.²⁹ Primer sequences are detailed in Table 1.

Table 1. Primer sequences in quantitative real-time polymerase chain reaction (qPCR)

Gene	Primer sequence	Amplicon size
<i>miR-497-5p</i>	F: 5'-ATCCAGTGC GTGTCGTG-3'	461
	R: 5'-TGCTCAGCAGC ACACTGT-3'	
<i>U6</i>	F: 5'-GCTTCGGCAGC A CATATACTAAAT-3'	91
	R: 5'-CGCTTACGA ATTGCGTGTCAT-3'	
<i>TFRC</i>	F: 5'-GGCTACTTGGGCTATTGTAAAGG-3'	156
	R: 5'-CAGTTTCTCCGACA ACTTCTCT-3'	
<i>GAPDH</i>	F: 5'-TGAAGGTCCGAGTCAACGGATT-3'	171
	R: 5'-CCTGGAAGATGGTGATGGGATT-3'	

Western blot

Cervical cancer cells in different transfection groups were lysed on ice for 30 min using a pre-cooled radioimmunoprecipitation reagent (Beyotime, Shanghai, China). The supernatant was removed and centrifuged at 14,000 rpm and 4°C, followed by collection. Total proteins were determined with a BCA protein concentration kit (RTP7102; Real-Times Biotechnology, Beijing, China). Next, protein samples (20 μg) were separated on a 10% sodium dodecyl-sulfate polyacrylamide gel electrophoresis (SDS-PAGE) and transferred onto

polyvinylidene fluoride (PVDF) membranes (Corning Inc., Corning, USA). Then, the membranes were blocked with 5% skimmed milk at room temperature for 2 h, and probed with monoclonal antibodies; rabbit anti-TFRC (ab214039, 1:1000; Abcam, Cambridge, UK), rabbit anti-GAPDH (ab181602, 1:10000; Abcam), rabbit anti-cleaved caspase-3 (ab32042, 1:500; Abcam), rabbit anti-cleaved caspase-9 (SAB4503337, 1:500; Merck, Rahway, USA), rabbit anti-E-cadherin (ab40772, 1:5000; Abcam), rabbit anti-N-cadherin (ab76011, 1:5000; Abcam), and rabbit anti-vimentin (ab92547, 1:5000; Abcam) overnight at 4°C. Membranes were rinsed 3 times (15 min/time) with phosphate-buffered saline (PBS) and Tween-20, after which they were cultured with goat anti-rabbit IgG H&L (HRP) (ab6721, 1:2000; Abcam) at room temperature for 1 h. Afterward, images were acquired using a chemiluminescence detection kit (Sigma-Aldrich, St. Louis, USA) in the darkroom. ImageJ software (National Institutes of Health, Bethesda, USA) was used for statistical analysis of the results.

MTT and colony formation assays

Cells were cultured in 96-well plates (5×10³ cells/well), and after transfection for 0, 24, 48, 72, and 96 h, 20 μL of 3-(4,5-dimethylthiazol-2-yl)-2,5-diphenyltetrazolium bromide (MTT) (5 g/L; Sigma-Aldrich) was added for another 4 h of cell incubation at 37°C. Then, 150 μL of dimethyl sulfoxide (DMSO) was supplemented to each well to dissolve crystal violet. Finally, a spectrophotometer was utilized to detect the absorbance at 570 nm.

The 6-well plates (5×10² cells/well) were recommended for cell seeding, and the culture medium was replaced every 3 days. After 10 days, the cells were rinsed twice with 1×PBS, followed by 20 min of 4% paraformaldehyde and 5 min of crystal violet. Five fields were selected under an optical microscope (model CKX53; Olympus Corp., Tokyo, Japan). The number of colonies was counted.

Cell migration and invasion assays

Mitomycin C (MedChemExpress, Monmouth Junction, USA) (10 μg/mL) was used to eliminate the influence of cell proliferation. The 24-well insert and polycarbonate membrane with 8.0-μm well (Millipore, Burlington, USA) was utilized for experiments. To assess cell migration, 5×10⁴ cells were inoculated to the upper chamber with serum-free medium, while the lower chamber was supplemented with 800 μL medium plus 10% FBS. Then, the cells were kept for 24 h in this medium. Regarding the cell invasion assessment, the transwell upper chamber was covered with 30 μL Matrigel (BD Biosciences, Franklin Lakes, USA) at first. Next, 1×10⁵ cells were inoculated as described above, followed by culturing for 24 h. Residues in the upper chamber were swabbed and cells outside the membrane were stained with 0.1% crystal violet. A microscope (model CKX53; Olympus Corp.) was used to observe 5 different fields of view.

Cell apoptosis and cell cycle analysis

Apoptosis was analyzed using a cell apoptosis kit (BD Biosciences) according to the manufacturer's instructions. First, the cells were prepared into a single-cell suspension, which was re-suspended with PBS after centrifugation. Then, the negative and positive control groups were prepared. For the assessment of cell apoptosis, propidium iodide (PI) and Annexin V were used to stain the cells, followed by flow cytometry using a FACSCanto™ II (BD Biosciences). To analyze the cell cycle, staining was conducted with PI only, followed by flow cytometry.

Dual-luciferase reporter gene assay

First, gene sequences of the 3'-untranslated region (3'-UTR) of wild-type (WT) or mutant (MUT) TFRC were cloned into pmir-GLO vector (Promega, Madison, USA), and named TFRC-WT and TFRC-MUT, respectively. The miR-497-5p mimic/NC mimic and TFRC-WT/TFRC-MUT vectors were transfected into cervical cancer cells with the use of Lipofectamine™ 2000 (Invitrogen). Then, luciferase activity was evaluated using a dual-luciferase reporter detection system (Promega).

Statistical analyses

All collected data were processed using GraphPad Prism v. 6.0 (GraphPad Software, San Diego, USA), while the “edgeR” package and “survival” package were processed with R software v. 4.0.2 (MathSoft, Cambridge, USA). All in vitro experiments were repeated 9 times. Due to the limited statistical sample size, which was insufficient for normal distribution, the data did not meet the assumption of normal distribution. Therefore, Mann–Whitney U tests were used to make the comparison between the 2 groups, a Kruskal–Wallis test was used to test the comparison between more than 2 groups, and Dunn's test was applied as a post hoc test. The Kaplan–Meier curve was utilized to conduct survival analysis, and Pearson correlation analysis was utilized to determine upstream miRNAs of the target gene. All data are expressed as mean \pm standard deviation ($M \pm SD$), with $p < 0.05$ representing statistical significance, $p < 0.01$ indicating a significant difference and $p < 0.001$ denoting an extremely significant difference.

Results

TFRC expression is significantly increased in cervical cancer cells

To identify the differentially expressed genes in cervical cancer, mRNAs in the TCGA database were categorized, with $|\log FC| > 1.5$ and false discovery rate (FDR) < 0.05 as cutoff standards. Through the differential expression

analysis conducted using the “edgeR” package, a total of 2956 DE mRNAs were obtained, among which 1274 genes were upregulated (red dots), 1682 genes were differentially downregulated (green dots), and the black dots represented genes with insignificant differences (Fig. 1A). Although previous studies have reported that concomitant upregulation of *TFRC* in various tumor tissues is associated with poor prognosis and facilitates cancer cell proliferation and metastasis,^{9,30} its role in cervical cancer is less understood. Therefore, *TFRC* was selected for follow-up investigations. The results of the differential expression analysis, as presented in Fig. 1B, revealed an increased *TFRC* expression in cervical cancer tissue compared to normal tissue ($p < 0.05$, Mann–Whitney U test). Meanwhile, clinical data demonstrated that *TFRC* expression displayed a significant difference in various clinical T/N stages with an increasing trend ($p < 0.01$, Kruskal–Wallis test; $p < 0.05$, Mann–Whitney U test) (Fig. 1C,D). The survival analysis further showed that the upregulation of *TFRC* in cervical cancer tissue influenced a patient's prognosis ($p < 0.050$, Mann–Whitney U test) (Fig. 1E), with the survival time of patients with decreased *TFRC* level being longer than those with increased *TFRC* expression. Relative to HcerEpic cells, *TFRC* expression was increased in Hela, SiHa, Caski, and C33A cells (Hela compared to HcerEpic: $p < 0.001$, SiHa compared to HcerEpic: $p < 0.001$, Caski compared to HcerEpic: $p < 0.01$, C33A compared to HcerEpic: $p < 0.05$, Kruskal–Wallis test with Dunn's post hoc test) (Fig. 1F). Therefore, Hela and SiHa cell lines with relatively high *TFRC* levels were chosen for further functional experiments.

TFRC silencing contributes to attenuating cancer cell malignant phenotypes

To identify the impact of *TFRC* on cancer cells, sh-*TFRC* and sh-NC were transfected into Hela and SiHa cell lines. Transfection efficacy was verified using qPCR, showing that the *TFRC* level was significantly decreased in the sh-*TFRC* group ($p < 0.05$, Mann–Whitney U test) (Fig. 2A). To investigate whether *TFRC* expression affects cervical cell behaviors and phenotypes, several cell function experiments were introduced. Silencing *TFRC* restrained cervical cancer cell proliferation ($p < 0.05$, Mann–Whitney U test) (Fig. 2B), while colony formation assays demonstrated that silencing *TFRC* resulted in fewer colonies of Hela and SiHa cells relative to the sh-NC group ($p < 0.05$, Mann–Whitney U test) (Fig. 2C). To define the impact of *TFRC* expression on cell migration and invasion, a transwell assay was performed, showing that cell migration and invasion were significantly reduced in the sh-*TFRC* group compared to those in the sh-NC group ($p < 0.05$, Mann–Whitney U test) (Fig. 2D,E). Furthermore, the cell apoptosis assay illustrated that silencing *TFRC* significantly upregulated ($p < 0.05$, Mann–Whitney U test) the cell apoptosis rate (Fig. 2F). Considering the influence of *TFRC* on the cell cycle, flow cytometry was used to examine the cell cycle

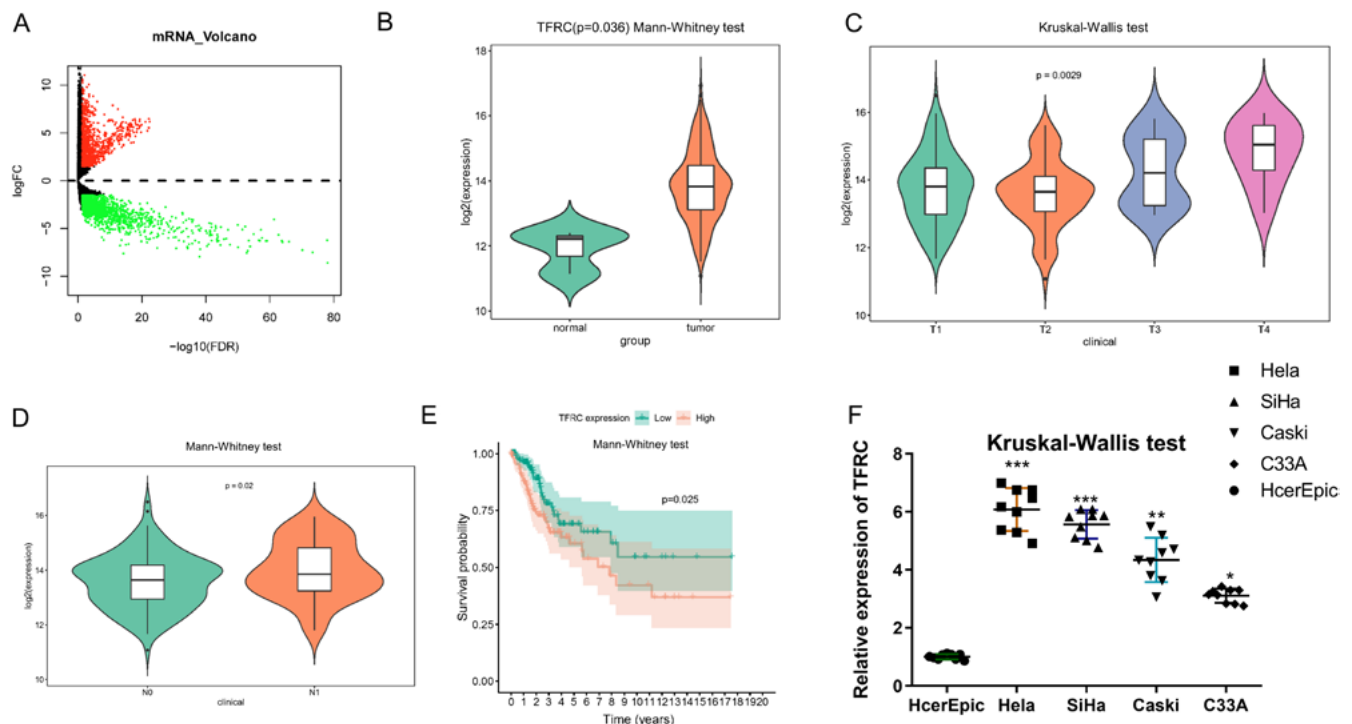


Fig. 1. Transferrin receptor (*TFRC*) level is increased in cervical cancer cells. A. Volcano map of differentially expressed (DE)mRNAs in normal and tumor samples in cervical cancer dataset (red dots: upregulated DE mRNAs, green dots: downregulated DE mRNAs); B. Violin plot of *TFRC* level in the normal ($n = 3$, green) and tumor ($n = 306$, red) samples (Mann–Whitney U test); C, D. Violin plot of *TFRC* level in varying T stages (T1–T4) (Kruskal–Wallis test) and varying N stages (N0, N1) (Mann–Whitney U test); E. Survival curves of high/low *TFRC* level on patient's prognosis (red line: high-*TFRC* level group; green line: low-*TFRC* level group (Mann–Whitney U test)); F. Quantitative real-time polymerase chain reaction (qPCR) measured *TFRC* expression in HcerEpic and Hela, SiHa, Caski, and C33A cells (Kruskal–Wallis test, Dunn's test was used for post-inspection)

* $p < 0.05$ indicated statistically significant values; ** $p < 0.01$ indicated a significant difference; *** $p < 0.001$ indicated an extremely significant difference.

status between the differentially transfected cell lines. Inhibiting the expression of *TFRC* could arrest the cell cycle in cervical cancer cells in the G0/G1 phase ($p < 0.05$, Mann–Whitney U test) (Fig. 2G). These findings highlighted that silencing *TFRC* hampered the progression of cervical cancer cell phenotype in vitro.

miR-497-5p inhibits the *TFRC* expression in cervical cancer cells

To screen potential upstream regulatory miRNAs for *TFRC*, miRNAs in the TCGA database were categorized, with $|\log FC| > 1.5$ and $FDR < 0.05$ set as cutoff standards. A differential analysis was conducted using the “edgeR” package, highlighting 128 DE miRNAs, among which 76 genes were upregulated (red dots), 52 genes were differentially downregulated (green dots), and the black dots represented miRNAs with insignificant differences (Fig. 3A). Next, the upstream regulatory miRNAs of *TFRC* were mined using bioinformatics databases. Predicted miRNAs overlapped with downregulated DE miRNAs, and thus we obtained 8 DE miRNAs with binding sites into *TFRC* (Fig. 3B). Then, the correlation analysis was conducted on *TFRC* and 8 DE miRNAs, and a negative correlation was found between *miR-497-5p* and *TFRC*, along with the highest coefficient ($p = -0.27$) (Fig. 3C). Through

bioinformatics analysis, we theorized that *miR-497-5p* level was lowered in cervical cancer tissue compared to normal tissue ($p < 0.001$, Mann–Whitney U test) (Fig. 3D). Therefore, *miR-497-5p* was selected for further analysis.

A binding site analysis demonstrated that *miR-497-5p* was a direct binding partner of *TFRC* (Fig. 3E). To investigate whether *miR-497-5p* targets *TFRC* by binding to its 3'UTR, WT or MUT *TFRC* luciferase reporter plasmid and *miR-497-5p* mimic or NC mimic were co-transfected into Hela and SiHa cells. The luciferase activity assay showed that luciferase activity of *TFRC*-WT in Hela and SiHa cell lines in the *miR-497-5p* mimic group was significantly reduced ($p < 0.05$, Mann–Whitney U test), and no substantial difference was observed in the *TFRC*-MUT group ($p > 0.05$, Mann–Whitney U test) (Fig. 3F). Furthermore, the upregulation of *miR-497-5p* significantly reduced *TFRC* mRNA ($p < 0.05$, Mann–Whitney U test) and protein levels, as assessed through qPCR and WB (Fig. 3G, H). Hence, it could be determined that *miR-497-5p* inhibited *TFRC* expression.

To investigate the influence of *miR-497-5p* on cervical cancer cells, a *miR-497-5p* overexpression cell line was established for cell function experiments. Western blot (WB) analysis revealed that when *miR-497-5p* was overexpressed, protein expression of apoptosis-related proteins, namely cleaved caspase-3 and cleaved caspase-9, was significantly elevated compared with the NC group

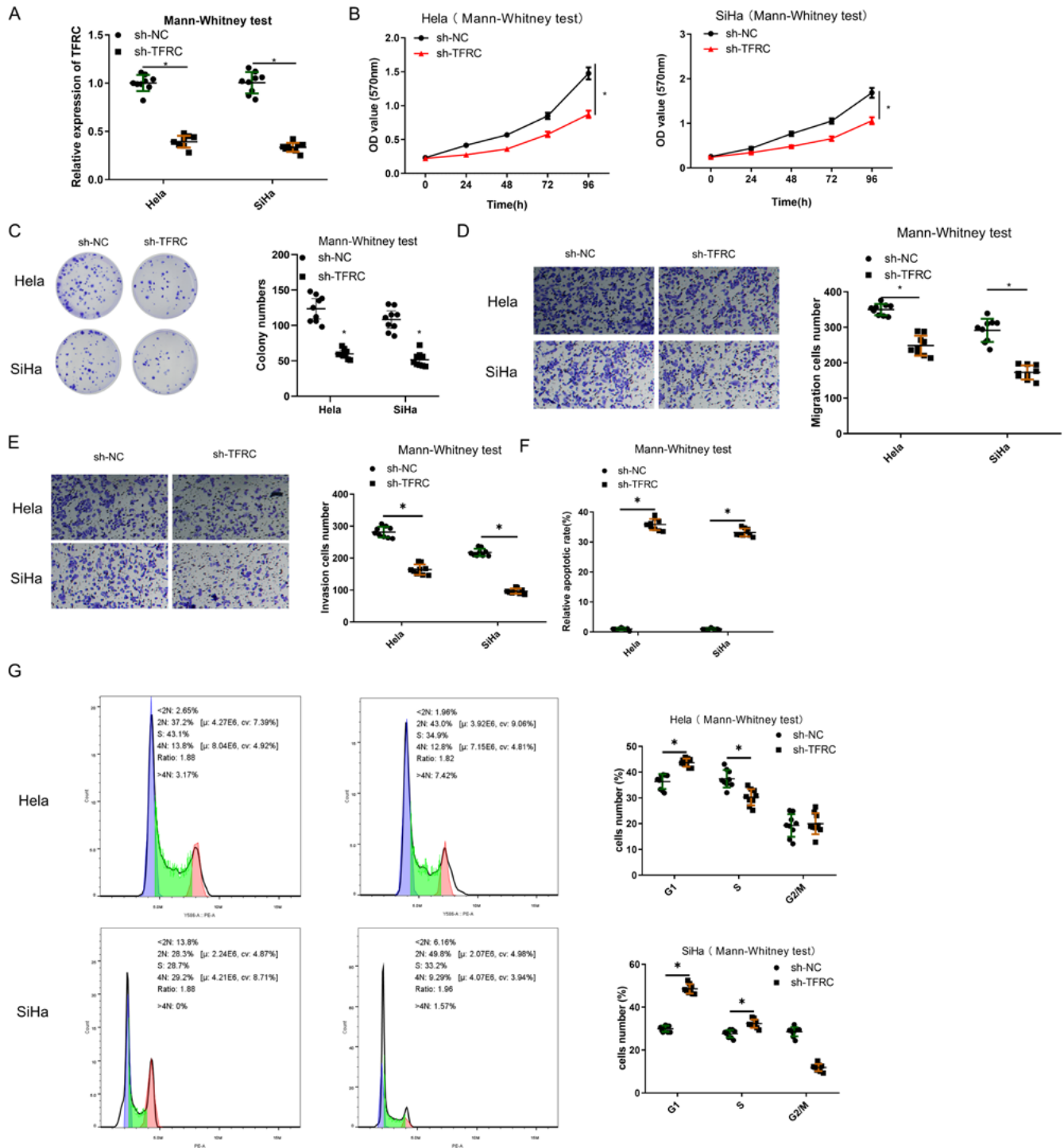


Fig. 2. Silencing transferrin receptor (TFRC) hinders cervical cancer cell phenotype progression. A. Transfection efficacy in HeLa and SiHa cells (Mann-Whitney U test); B. Proliferative property of cervical cancer cells (Mann-Whitney U test); C. Cell colony formation of cervical cancer cells (Mann-Whitney U test); D,E. Cell migration and invasion in various treatment groups (100x) (Mann-Whitney U test); F. Apoptosis rate of cervical cancer cells in varying transfection groups (Mann-Whitney U test); G. Cell cycle in differently transfected cell lines (Mann-Whitney U test)

* $p < 0.05$ indicated statistically significant values; OD – optical density.

(Supplementary Fig. 1). The transwell assay further demonstrated that the overexpression of miR-497-5p inhibited cervical cell migration and invasion compared with the NC group ($p < 0.05$, Mann-Whitney U test) (Supplementary Fig. 2). Next, we detected levels of epithelial-mesenchymal transition (EMT)-related proteins using WB, showing that

the overexpression of miR-497-5p hampered N-cadherin and vimentin protein levels, and fostered E-cadherin protein levels compared with the NC group ($p < 0.050$, Mann-Whitney U test) (Supplementary Fig. 3). These results illustrated that miR-497-5p could hamper migration and invasion of cervical cancer cells, but foster cell apoptosis.

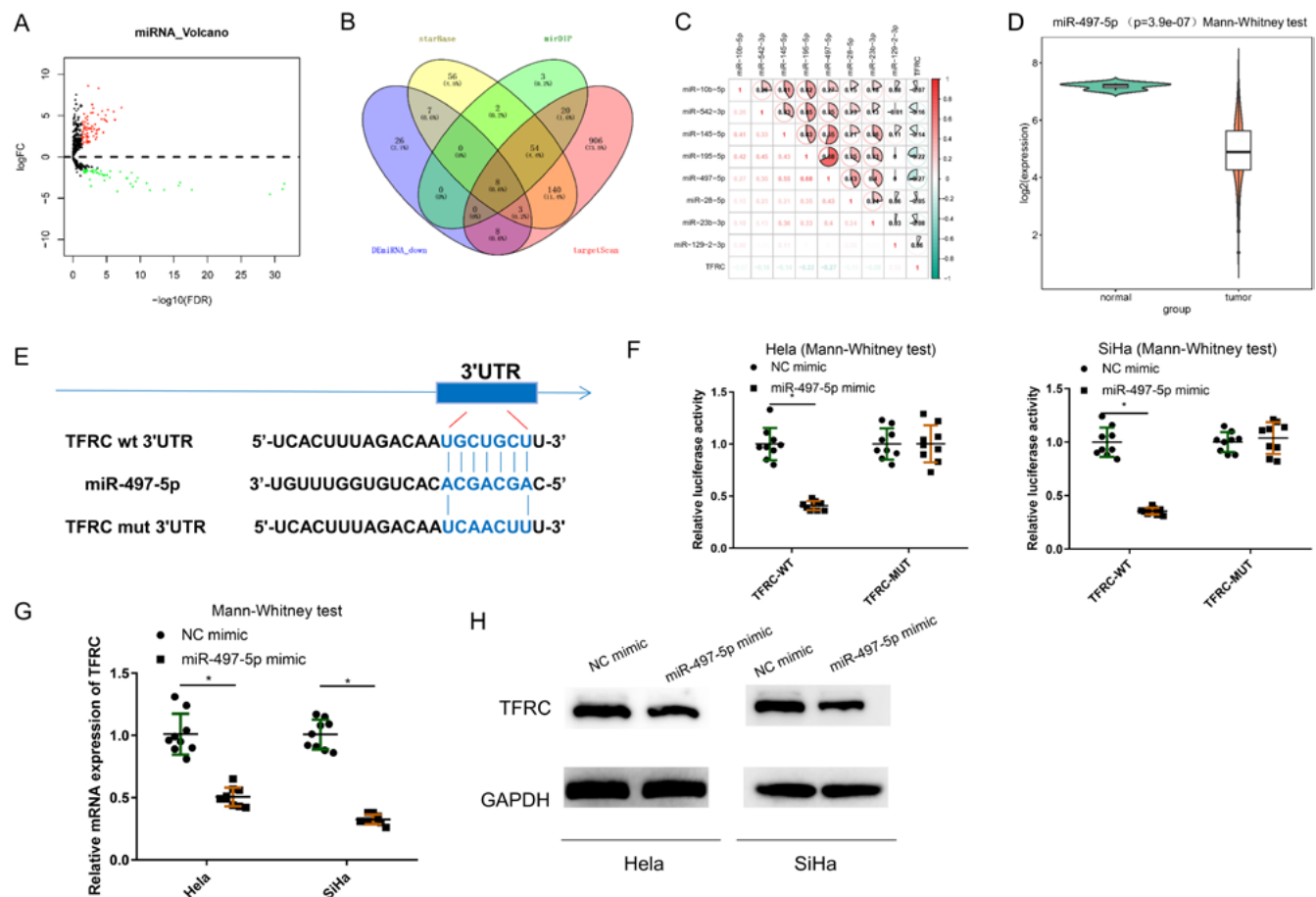


Fig. 3. MicroRNA-497-5p (miR-497-5p) hampers transferrin receptor (TFRC) in cervical cancer cells. **A.** Volcano map of differentially expressed (DE) miRNAs in normal and tumor groups in cervical cancer dataset (red dots: upregulated DE miRNAs, green dots: downregulated DE miRNAs); **B.** Venn diagram of the predicted upstream miRNAs of TFRC and downregulated DE miRNAs; **C.** Pearson correlation analysis of 8 upstream regulatory miRNAs and TFRC; **D.** miR-497-5p level in normal (n = 3, green) and tumor (n = 309, red) samples (Mann–Whitney U test); **E.** Binding sites of TFRC and miR-497-5p; **F.** Luciferase activity of HeLa and SiHa cells (Mann–Whitney U test); **G,H.** TFRC mRNA and protein levels in HeLa and SiHa cells (Mann–Whitney U test)

*p < 0.05 indicated statistically significant values.

miR-497-5p hampers malignant progression of cervical cancer cells by downregulating TFRC

To determine whether miR-497-5p modulates the development of cervical cancer cells via TFRC, a miR-497-5p mimic was utilized to upregulate miR-497-5p. Simultaneously, the miR-497-5p mimic and oe-TFRC were co-transfected into cervical cancer cells. Through qRT-PCR and WB, it was observed that the upregulation of miR-497-5p decreased TFRC expression compared to the NC mimic+oe-NC group, and TFRC level was elevated in the miR-497-5p mimic+oe-TFRC group compared with the miR-497-5p mimic group (p < 0.05, Mann–Whitney U test) (Fig. 4A,B). The MTT and colony formation assay unveiled that proliferation and colony formation of HeLa and SiHa cells were hindered by transfecting the miR-497-5p mimic, but the inhibitory impact was partially eliminated by co-transfecting with oe-TFRC (p < 0.05, Mann–Whitney U test) (Fig. 4C,D). Moreover, migratory and invasive properties were weakened in cervical cancer cells that

overexpressed miR-497-5p compared with the NC group, whereas TFRC overexpression reversed this inhibitory effect and returned to NC group levels (p < 0.05, Mann–Whitney U test) (Fig. 4E,F). Moreover, flow cytometry showed that increased miR-497-5p resulted in increased apoptosis of HeLa and SiHa cells compared with the NC group, but simultaneous overexpression of miR-497-5p and TFRC reduced the apoptosis (p < 0.05, Mann–Whitney U test) (Fig. 4G). Similarly, miR-497-5p facilitated cell cycle arrest in the G0/G1 phase, but the cell cycle was restored in the NC group by additional transfection of oe-TFRC (p < 0.05, Mann–Whitney U test) (Fig. 4H). Together, these findings revealed that TFRC modulated cervical cancer cell progression via the restraining influence of miR-497-5p.

Discussion

Patients with advanced cervical adenocarcinoma are largely incurable due to local recurrence and metastatic diffusion.³¹ As reported previously, many mRNAs are

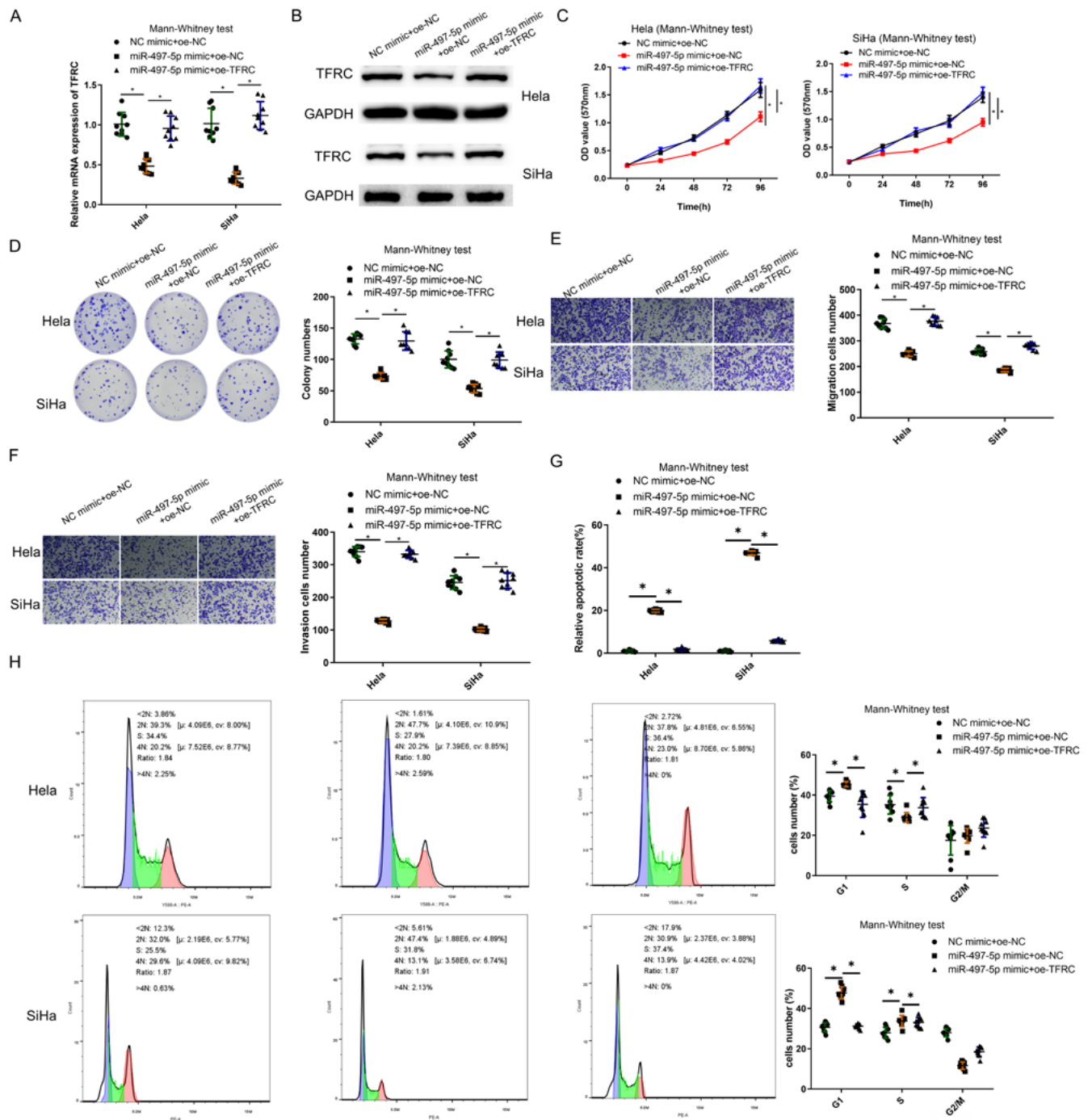


Fig. 4. MicroRNA-497-5p (*miR-497-5p*) represses cell phenotype progression in cervical cancer through transferrin receptor (*TFRC*) downregulation. A,B. *TFRC* mRNA and protein levels in cervical cancer cells (HeLa and SiHa) (Mann-Whitney U test); C. Cell proliferation in varying groups (Mann-Whitney U test); D. Colony formation of cervical cancer cells in various treatment groups (Mann-Whitney U test); E,F. Cell migration and invasion in various treatment groups (100x) (Mann-Whitney U test); G. Cell apoptosis in various treatment groups (Mann-Whitney U test); H. Cell cycle statuses in various groups (Mann-Whitney U test)

*p < 0.05 indicated statistically significant values; OD – optical density.

aberrantly expressed in cervical cancer and are implicated in tumorigenesis and progression.³² Of note, exploring the potential mechanism of cervical cancer may lead to its early diagnosis and effective therapy.³³ Transferrin receptor is present in almost all mammalian cells.³⁴ Herein, *TFRC* expression data in cervical cancer were analyzed for the mechanism of *TFRC* dysregulation in the pathogenesis

of the disease, finding that *TFRC* was upregulated, and silencing *TFRC* repressed the progression of cervical cancer cell phenotype. Previous studies have uncovered that *TFRC* is increased in both colon and lung cancers. Specifically, Fu et al. highlighted that TFR1 was significantly increased and was essential in the malignant progression of colorectal cancer.³⁵ Furthermore, Whitney et al. confirmed that

TFRC was significantly increased in NSCLC.³⁶ Our work is concordant with an earlier report that compared the up-regulation of *TFRC* in cervical cancers to adjacent non-tumor tissue and correlated these results to progression stages, tumor status and lymph node involvement.³⁷ These findings show that *TFRC* may function as a direct and indirect target for the administration of therapeutics, presenting a potential prospect in treating cancer cell malignant progression.

This work uncovered the mechanism of *miR-497-5p* modulating *TFRC* in cervical cancer cells. Earlier studies have shown that *miR-497-5p*, *miR-320* and *miR-210* target *TFRC*.^{38,39} Herein, we have demonstrated that *TFRC* was a direct target of *miR-497-5p*. Moreover, through bioinformatics analysis, a negative link between *miR-497-5p* and *TFRC* was uncovered. Our finding is congruous with previous evidence stating that the expression of *miR-497-5p* is reduced in gastric cancer,²⁶ while Li et al. proposed that *miR-497-5p* is significantly decreased in NSCLC.⁴⁰ Most importantly, increased *miR-497-5p* expression decreased *TFRC* in cervical cancer cells, while *miR-497-5p* and *TFRC* overexpression restored the repressive influence of overexpressing *miR-497-5p* on cervical cancer. This result was also supported by Chen et al.⁴¹ Given that *miR-497-5p* targets *TFRC* to repress cervical cancer tumorigenesis and progression, it may represent a feasible therapeutic target for cervical cancer patients.

Limitations

While the findings of the study are promising, an analysis of these aspects in animal models and clinical trials would be valuable. Therefore, future research will focus on the mechanism of the *miR-497-5p/TFRC* axis in cervical cancer from multiple perspectives in order to offer a theoretical foundation for potential therapies.

Conclusions

Transferrin receptor knockdown could inhibit the proliferation, migration and invasion of cervical cancer cells while promoting apoptosis. Regarding the regulatory mechanism, concomitant upregulation of *TFRC* is caused by decreased *miR-497-5p* level, while the upregulation of *miR-497-5p* repressed the malignant phenotype of cervical cancer by modulating *TFRC*. This work has contributed to proposing more therapeutic regimens for cervical cancer.

Supplementary data

The supplementary materials are available at <https://doi.org/10.5281/zenodo.8032200>. The package contains the following files:

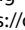
Supplementary Fig. 1. Expression of apoptosis-related proteins, cleaved caspase-3 and cleaved caspase-9, as assayed by WB.

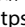
Supplementary Fig. 2. Cell migration and invasion abilities evaluated using transwell assay (Mann–Whitney U test).


Supplementary Fig. 3. Changes in expression of EMT-related proteins evaluated using WB (Mann–Whitney U test; **p* < 0.050 represents statistically significant values).


ORCID iDs

Xiangming Fang  <https://orcid.org/0000-0003-0757-2274>

Pei Hu  <https://orcid.org/0009-0004-0576-367X>

Ying Gao  <https://orcid.org/0009-0005-5529-8611>

Chunqiao Chen  <https://orcid.org/0009-0008-4882-9017>

Jianqing Xu  <https://orcid.org/0000-0001-7022-5369>

References

1. Ji X, Guo H, Yin S, Du H. miR-139-5p functions as a tumor suppressor in cervical cancer by targeting TCF4 and inhibiting Wnt/β-catenin signaling. *Oncotargets Ther.* 2019;12:7739–7748. doi:10.2147/OTT.S215796
2. Fu K, Zhang L, Liu R, Shi Q, Li X, Wang M. MiR-125 inhibited cervical cancer progression by regulating VEGF and PI3K/AKT signaling pathway. *World J Surg Oncol.* 2020;18(1):115. doi:10.1186/s12957-020-01881-0
3. Cohen PA, Jhingran A, Oaknin A, Denny L. Cervical cancer. *Lancet.* 2019;393(10167):169–182. doi:10.1016/S0140-6736(18)32470-X
4. Isik A, Wysocki AP, Memiş U, Sezgin E, Yezhikova A, Islambekov Y. Factors associated with the occurrence and healing of umbilical pilonidal sinus: A rare clinical entity. *Adv Skin Wound Care.* 2022;35(8):1–4. doi:10.1097/01.ASW.0000833608.27136.d1
5. Isik A, Soran A, Grasi A, Barry N, Sezgin E. Lymphedema after sentinel lymph node biopsy: Who is at risk? *Lymphat Res Biol.* 2022;20(2):160–163. doi:10.1089/lrb.2020.0093
6. Hill EK. Updates in cervical cancer treatment. *Clin Obstet Gynecol.* 2020;63(1):3–11. doi:10.1097/GRF.0000000000000507
7. Chopra S, Gupta M, Mathew A, et al. Locally advanced cervical cancer: A study of 5-year outcomes. *Indian J Cancer.* 2018;55(1):45–49. doi:10.4103/ijc.IJC_428_17
8. Bose CK. Balstilimab and other immunotherapy for recurrent and metastatic cervical cancer. *Med Oncol.* 2022;39(4):47. doi:10.1007/s12032-022-01646-7
9. Huang Y, Huang J, Huang Y, et al. TFRC promotes epithelial ovarian cancer cell proliferation and metastasis via up-regulation of AXIN2 expression. *Am J Cancer Res.* 2020;10(1):131–147. PMID:32064157.
10. Cui P, Dai X, Liu R, Cao H. LncRNA LINC00888 upregulation predicts a worse survival of laryngeal cancer patients and accelerates the growth and mobility of laryngeal cancer cells through regulation of miR-378g/TFRC. *J Biochem Mol Toxicol.* 2021;35(10):e22878. doi:10.1002/jbt.22878
11. Yang C, Li J, Guo Y, et al. Role of TFRC as a novel prognostic biomarker and in immunotherapy for pancreatic carcinoma. *Front Mol Biosci.* 2022;9:756895. doi:10.3389/fmolb.2022.756895
12. Muhammad JS, Bajbouj K, Shafarin J, Hamad M. Estrogen-induced epigenetic silencing of *FTL1* and *TFRC* genes reduces liver cancer cell growth and survival. *Epigenetics.* 2020;15(12):1302–1318. doi:10.1080/15592294.2020.1770917
13. Kim H, Villareal LB, Liu Z, et al. Transferrin receptor-mediated iron uptake promotes colon tumorigenesis. *Adv Sci (Weinh).* 2023;10(10):e2207693. doi:10.1002/advs.202207693
14. Zhang J, Chen S, Wei S, et al. CircRAPGEF5 interacts with RBFOX2 to confer ferroptosis resistance by modulating alternative splicing of TFRC in endometrial cancer. *Redox Biol.* 2022;57:102493. doi:10.1016/j.redox.2022.102493
15. Shen Y, Li X, Dong D, Zhang B, Xue Y, Shang P. Transferrin receptor 1 in cancer: A new sight for cancer therapy. *Am J Cancer Res.* 2018; 8(6):916–931. PMID:30034931. PMCID:PMC6048407.
16. He B, Zhao Z, Cai Q, et al. miRNA-based biomarkers, therapies, and resistance in cancer. *Int J Biol Sci.* 2020;16(14):2628–2647. doi:10.7150/ijbs.47203
17. Menon A, Abd-Aziz N, Khalid K, Poh CL, Naidu R. miRNA: A promising therapeutic target in cancer. *Int J Mol Sci.* 2022;23(19):11502. doi:10.3390/ijms231911502

18. Mou T, Xie F, Zhong P, et al. miR-345-5p functions as a tumor suppressor in pancreatic cancer by directly targeting CCL8. *Biomed Pharmacother*. 2019;111:891–900. doi:10.1016/j.biopha.2018.12.121
19. Petrovic N, Ergun S. miRNAs as potential treatment targets and treatment options in cancer. *Mol Diagn Ther*. 2018;22(2):157–168. doi:10.1007/s40291-017-0314-8
20. Liang Z, Yang Y, Sun X, et al. Integrated analysis of microRNA and mRNA expression profiles in the fat bodies of MbMNPV-infected *Helicoverpa armigera*. *Viruses*. 2022;15(1):19. doi:10.3390/v15010019
21. Lu M, Gao Q, Wang Y, Ren J, Zhang T. LINC00511 promotes cervical cancer progression by regulating the miR-497-5p/MAPK1 axis. *Apoptosis*. 2022;27(11–12):800–811. doi:10.1007/s10495-022-01768-3
22. Wang L, Guo J, Zhou J, Wang D, Kang X, Zhou L. NF- κ B maintains the stemness of colon cancer cells by downregulating miR-195-5p/497-5p and upregulating MCM2. *J Exp Clin Cancer Res*. 2020;39(1):225. doi:10.1186/s13046-020-01704-w
23. Liu C, Bordeaux A, Hettich S, Han S. MicroRNA-497-5p functions as a modulator of apoptosis by regulating metadherin in ovarian cancer. *Cell Transplant*. 2020;29:096368971989706. doi:10.1177/0963689719897061
24. Huang X, Wang L, Liu W, Li F. MicroRNA-497-5p inhibits proliferation and invasion of non-small cell lung cancer by regulating FGF2. *Oncol Lett*. 2019;17(3):3425–3431. doi:10.3892/ol.2019.9954
25. Zheng S, Hou J, Chang Y, Zhao D, Yang H, Yang J. CircRNA Circ-CCND1 aggravates hepatocellular carcinoma tumorigenesis by regulating the miR-497-5p/HMGA2 axis. *Mol Biotechnol*. 2022;64(2):178–186. doi:10.1007/s12033-021-00391-y
26. Feng L, Cheng K, Zang R, Wang Q, Wang J. miR-497-5p inhibits gastric cancer cell proliferation and growth through targeting PDK3. *Biosci Rep*. 2019;39(9):BSR20190654. doi:10.1042/BSR20190654
27. Hu J, Peng X, Du W, Huang Y, Zhang C, Zhang X. circSLC6A6 sponges miR-497-5p to promote endometrial cancer progression via the PI4KB/Hedgehog axis. *J Immunol Res*. 2021;2021:5512391. doi:10.1155/2021/5512391
28. Fridrichova I, Kalinkova L, Karhanek M, et al. miR-497-5p decreased expression associated with high-risk endometrial cancer. *Int J Mol Sci*. 2020;22(1):127. doi:10.3390/ijms22010127
29. Liu S, Wang L, Zhang R. Corylin suppresses metastasis of breast cancer cells by modulating miR-34c/LINC00963 target. *Libyan J Med*. 2021;16(1):1883224. doi:10.1080/19932820.2021.1883224
30. Ye J, Wang Z, Chen X, et al. YTHDF1-enhanced iron metabolism depends on TFRC m⁶A methylation. *Theranostics*. 2020;10(26):12072–12089. doi:10.7150/thno.51231
31. Liu X, Zhou Y, Ning YE, Gu H, Tong Y, Wang N. MiR-195-5p inhibits malignant progression of cervical cancer by targeting YAP1. *Onco Targets Ther*. 2020;13:931–944. doi:10.2147/OTT.S227826
32. Li N, Yu K, Lin Z, Zeng D. Identifying a cervical cancer survival signature based on mRNA expression and genome-wide copy number variations. *Exp Biol Med (Maywood)*. 2022;247(3):207–220. doi:10.1177/15353702211053580
33. Díaz-González SDM, Deas J, Benítez-Boijseaneau O, et al. Utility of microRNAs and siRNAs in cervical carcinogenesis. *Biomed Res Int*. 2015;2015:374924. doi:10.1155/2015/374924
34. Thorstensen K, Romslo I. The transferrin receptor: Its diagnostic value and its potential as therapeutic target. *Scand J Clin Lab Invest Suppl*. 1993;215:113–120. doi:10.3109/00365519309090703
35. Fu Y, Lin L, Xia L. MiR-107 function as a tumor suppressor gene in colorectal cancer by targeting transferrin receptor 1. *Cell Mol Biol Lett*. 2019;24:31. doi:10.1186/s11658-019-0155-z
36. Whitney JF, Clark JM, Griffin TW, Gautam S, Leslie KO. Transferrin receptor expression in nonsmall cell lung cancer. Histopathologic and clinical correlates. *Cancer*. 1995;76(1):20–25. doi:10.1002/1097-0142(19950701)76:1<20::AID-CNCR2820760104>3.0.CO;2-3
37. Xu X, Liu T, Wu J, Wang Y, Hong Y, Zhou H. Transferrin receptor-involved HIF-1 signaling pathway in cervical cancer. *Cancer Gene Ther*. 2019;26(11–12):356–365. doi:10.1038/s41417-019-0078-x
38. Schaar DG, Medina DJ, Moore DF, Strair RK, Ting Y. miR-320 targets transferrin receptor 1 (CD71) and inhibits cell proliferation. *Exp Hematol*. 2009;37(2):245–255. doi:10.1016/j.exphem.2008.10.002
39. Yoshioka Y, Kosaka N, Ochiya T, Kato T. Micromanaging iron homeostasis: Hypoxia-inducible micro-RNA-210 suppresses iron homeostasis-related proteins. *J Biol Chem*. 2012;287(41):34110–34119. doi:10.1074/jbc.M112.356717
40. Li G, Wang K, Wang J, Qin S, Sun X, Ren H. miR-497-5p inhibits tumor cell growth and invasion by targeting SOX5 in non-small-cell lung cancer. *J Cell Biochem*. 2019;120(6):10587–10595. doi:10.1002/jcb.28345
41. Chen Y, Du J, Wang Y, et al. MicroRNA-497-5p induces cell cycle arrest of cervical cancer cells in S phase by targeting CBX4. *Onco Targets Ther*. 2019;12:10535–10545. doi:10.2147/OTT.S210059